Advances in Atmospheric Sciences
Impact Factor: 5.8
E-alert
ISSN 0256-1530
CN 11-1925/O4

CAS–ESM2.0 Successfully Reproduces Historical Atmospheric CO_2 in a Coupled Carbon–Climate Simulation

Jiawen ZHU, Juanxiong HE, Duoying JI, Yangchun LI, He ZHANG, Minghua ZHANG, Xiaodong ZENG, Kece FEI, Jiangbo JIN

Citation: Zhu, J. W., and Coauthors 2023: CAS–ESM2.0 Successfully Reproduces Historical Atmospheric CO_2 in a Coupled CarbonClimate Simulation, *Adv. Atmos. Sci.*, In press. doi: 10.1007/s00376–023–3172–9.

View online: https://doi.org/10.1007/s00376–023–3172–9

ADVANCES IN ATMOSPHERIC SCIENCES, 2023

• News & Views •

CAS-ESM2.0 Successfully Reproduces Historical Atmospheric CO_2 in a Coupled Carbon–Climate Simulation

Jiawen ZHU[1,2], Juanxiong HE[*1], Duoying JI[3], Yangchun LI[4,6], He ZHANG[1], Minghua ZHANG[5], Xiaodong ZENG[1,2,6], Kece FEI[1], and Jiangbo JIN[1]

[1]*International Center for Climate and Environment Sciences*, *Institute of Atmospheric Physics*, *Chinese Academy of Sciences*, *Beijing* 100029, *China*

[2]*Collaborative Innovation Center on Forecast and Evaluation of Meteorological Disasters (CIC-FEMD)*, *Nanjing University of Information Science & Technology*, *Nanjing* 210044, *China*

[3]*College of Global Change and Earth System Science*, *Beijing Normal University*, *Beijing* 100875, *China*

[4]*State Key Laboratory of Atmospheric Boundary Layer Physics and Atmospheric Chemistry Institute of Atmospheric Physics*, *Chinese Academy of Sciences*, *Beijing* 100029, *China*

[5]*School of Marine and Atmospheric Sciences*, *Stony Brook University*, *NY* 11790, *USA*

[6]*University of Chinese Academy of Sciences*, *Beijing* 100049, *China*

(Received 30 July 2023; revised 4 September 2023; accepted 14 September 2023)

ABSTRACT

The atmospheric carbon dioxide (CO_2) concentration has been increasing rapidly since the Industrial Revolution, which has led to unequivocal global warming and crucial environmental change. It is extremely important to investigate the interactions among atmospheric CO_2, the physical climate system, and the carbon cycle of the underlying surface for a better understanding of the Earth system. Earth system models are widely used to investigate these interactions via coupled carbon–climate simulations. The Chinese Academy of Sciences Earth System Model version 2 (CAS-ESM2.0) has successfully fixed a two-way coupling of atmospheric CO_2 with the climate and carbon cycle on land and in the ocean. Using CAS-ESM2.0, we conducted a coupled carbon–climate simulation by following the CMIP6 proposal of a historical emissions-driven experiment. This paper examines the modeled CO_2 by comparison with observed CO_2 at the sites of Mauna Loa and Barrow, and the Greenhouse Gases Observing Satellite (GOSAT) CO_2 product. The results showed that CAS-ESM2.0 agrees very well with observations in reproducing the increasing trend of annual CO_2 during the period 1850–2014, and in capturing the seasonal cycle of CO_2 at the two baseline sites, as well as over northern high latitudes. These agreements illustrate a good ability of CAS-ESM2.0 in simulating carbon–climate interactions, even though uncertainties remain in the processes involved. This paper reports an important stage of the development of CAS-ESM with the coupling of carbon and climate, which will provide significant scientific support for climate research and China's goal of carbon neutrality.

Key words: CAS-ESM, atmospheric CO_2, coupled carbon–climate simulation, emissions-driven CMIP6 experiment

Citation: Zhu, J. W., and Coauthors, 2023: CAS-ESM2.0 successfully reproduces historical atmospheric CO_2 in a coupled carbon–climate simulation. *Adv. Atmos. Sci.*, https://doi.org/10.1007/s00376-023-3172-9.

1. Introduction

Carbon dioxide (CO_2) is an important greenhouse gas in the atmosphere of Earth. The atmospheric CO_2 concentration has been enhancing rapidly since the Industrial Revolution (IPCC, 2021). Observations show that the atmospheric CO_2 concentration in 2019 was 410.07 ± 0.10 ppm (parts per million), which was an increase of 47.5% relative to the value of 278.00 ± 5.00 ppm in 1750. The increase in atmospheric CO_2 can have remarkable effects on the global climate and environment, including warming of the climate through the greenhouse gas effect and stimulation of plant photosynthesis through fer-

* Corresponding author: Juanxiong HE
Email: hejx@mail.iap.ac.cn

tilization effects. Changes in atmospheric CO_2 and its effects are a key subject of global climate and environmental research.

Atmospheric CO_2 has strong spatiotemporal inhomogeneity, even though it is a well-mixed gas. Moreover, it shows clear seasonal variation, especially over northern high latitudes, with lower values in summer and higher values in winter, which is mainly driven by terrestrial ecosystems (Forkel et al., 2016). Satellite observations show that the seasonal amplitude of atmospheric CO_2 exceeds 10 ppm in the Northern Hemisphere (Ying et al., 2019). These findings have been confirmed by site observations reporting values exceeding 15 ppm at Point Barrow (71.32°N, 156.6°W) (Forkel et a., 2016) and values reaching 70 ppm in urban areas (Feng et al., 2018). Site observations also show an increase in the seasonal amplitude of atmospheric CO_2 in the past several decades, with a value of 50% north of 45°N (Graven et al., 2013). In terms of spatial distribution, the CO_2 concentration is higher in the Northern Hemisphere (Ying et al., 2019) and in regions with more human activities (Feng et al., 2018). These various line of evidence all point to the fact that the spatiotemporal variation of atmospheric CO_2 is very large and cannot be ignored.

Earth system models comprise interactions between the physical climate system and the carbon cycle at multiple spatiotemporal scales. They have been used widely to investigate the changes in atmospheric CO_2 concentration and its interactions with climate. Earth system models from many countries have participated in phase 6 of the Coupled Model Intercomparison Project (CMIP6). CMIP6 generally proposes two kinds of simulations with respect to CO_2: emissions-driven runs and concentration-driven runs (Eyring et al., 2016). In emissions-driven runs, atmospheric CO_2 is driven by anthropogenic emissions and interacts with carbon cycles on land and in the ocean. These runs request that models must have the ability to calculate atmospheric CO_2 concentrations. In concentration-driven runs, the atmospheric CO_2 concentration is prescribed, so it is not impacted by carbon cycles on land and in the ocean. As such, it is relatively more complicated and challenging for models to conduct emissions-driven runs than concentration-drive runs. For example, thus far, only 13 models have submitted historical emissions-driven runs to CMIP6, but 64 models have submitted historical concentration-driven runs. Therefore, many challenges and uncertainties remain for Earth system models to conduct fully coupled emissions-driven simulations of atmospheric CO_2.

The Chinese Academy of Sciences Earth System Model (CAS-ESM) has been continuously developed over the past several decades. The latest version, version 2, of CAS-ESM has completed the CMIP6 DECK (Diagnosis, Evaluation, and Characterization of Klima) simulations (concentration-driven runs) and submitted the results to CMIP6 (Zhang et al., 2020). Now, we have made a further development of CAS-ESM2.0 to fix a two-way coupling among the atmospheric CO_2, physical climate system, and carbon cycle on land and in the ocean. In this way, CAS-ESM2.0 can simulate CO_2–carbon–climate interactions and calculate the atmospheric CO_2 by itself. Using this version of CAS-ESM2.0, we conducted a coupled carbon–climate simulation following CMIP6's proposed historical emissions-driven experiment.

The objective of this paper is to introduce the coupling process and to report on the preliminary results of the modeled CO_2. Following this introduction, section 2 introduces the carbon cycles in CAS-ESM2.0, followed in section 3 by an introduction to the experimental design, data, and methods. Section 4 compares the modeled CO_2 to multiple sources of observed CO_2. Some discussion and a future outlook are provided in section 5, followed by an overall summary of this work in section 6.

2. Model description

The second version of CAS-ESM (CAS-ESM2.0) was released in 2020. Zhang et al. (2020) reported the model details and the climate simulation performance. This paper focuses on describing the model's coupled climate–carbon interactions and its performance with regard to CO_2 simulation. Figure 1 shows the CAS-ESM2.0 framework used in this study. We used the same components as those in Zhang et al. (2020) and turned on the Dynamic Global Vegetation Model (IAP DGVM; Zeng et al., 2014) and the ocean biogeochemical model (IAP OBGCM; Xu et al., 2013).

To conduct the coupled carbon–climate simulation, we first added CO_2 as a new dry-air tracer in our fifth-generation Atmospheric General Circulation Model (IAP AGCM5.0). Then, we made a two-way coupling between the atmospheric CO_2 and carbon fluxes on land and in the ocean. IAP AGCM5.0 describes the change in CO_2 in the horizontal and vertical directions, and these CO_2 changes are affected by net carbon fluxes from the land and ocean. Meanwhile, the bottom layer of CO_2 is transferred to the land and ocean components, and influences their calculations of carbon fluxes.

The land component, the Common Land Model (CoLM), obtains the value of CO_2 from the bottom layer of the atmosphere and uses it to calculate the photosynthesis (Ji et al., 2014). In this way, atmospheric CO_2 is partially absorbed. Conversely, the land component releases CO_2 to the atmosphere via plant autotrophic respiration and heterotrophic respiration—processes described in IAP DGVM (Zeng et al., 2014). IAP DGVM also includes modules describing carbon allocations among leaves, stems and roots, carbon turnover into above- and belowground litter pools, and plant establishment and mortality. IAP DGVM has been coupled to CAS-ESM2.0 and shows good ability in reproducing terrestrial carbon fluxes and spatial distributions of natural vegetation (Zhu et al., 2018). In addition, the process-based fire parameterization of intermediate com-

plexity in IAP DGVM can reasonably capture the global burned area and accurately estimate fire carbon emissions (Li et al., 2012). The fire carbon emissions are included and released to the atmosphere in this study.

The ocean biogeochemical model (IAP OBGCM) describes the air–sea CO_2 exchange process at the sea surface and the carbon biogeochemical cycle in the interior ocean (Xu et al., 2013). The uptake of atmospheric CO_2 is driven by the difference in the partial pressure of CO_2 between the atmosphere and the ocean. The sea surface water partial pressure of CO_2 is controlled by the sea surface temperature, salinity, concentrations of dissolved inorganic carbon, and total alkalinity. Dissolved inorganic carbon and total alkalinity are affected by biological processes. Biological production is a function of the concentrations of nutrients, such as phosphate and dissolved iron, water temperature, and light intensity in this model. As a product of biological production, the particulate organic matter transports carbon into the interior ocean quickly.

3. Experimental design, data and methods

3.1. *Experimental design*

We conducted two types of emission-driven experiments following the CMIP6 proposal (Table 1). The first one is the preindustrial control experiment (esm_piControl), in which anthropogenic CO_2 emissions are prescribed to be zero. In esm_piControl, CAS-ESM2.0 calculated the atmospheric CO_2 concentration via a two-way coupling with the carbon cycle in the ocean and on land. This setup is different to the concentration-driven preindustrial experiment in which the atmospheric CO_2 concentration is prescribed and not affected by the carbon cycle of the underlying surface. We ran esm_piControl for 550 years and achieved a near-equilibrium state in which the drifting of global mean atmospheric CO_2 was 0.05 ppm yr^{-1} near the end of the run. This drifting illustrates that our model is not yet ready to be used for long-timescale simulations—for example, the glacial–interglacial cycle. Therefore, we conducted a historical experiment (esm_historical) covering the period 1850–2014. The esm_historical experiment branched from year 514 of esm_piControl to obtain an appropriate starting value for CO_2 (284.742 ppm). In esm_historical, the CO_2 concentration is also calculated by CAS-ESM2.0, and the anthropogenic CO_2 emissions are input data from CMIP6, including emissions from fossil fuel combustion and land-use change (https://esgf-node.llnl.gov/search/input4mips/) during the period 1850–2014.

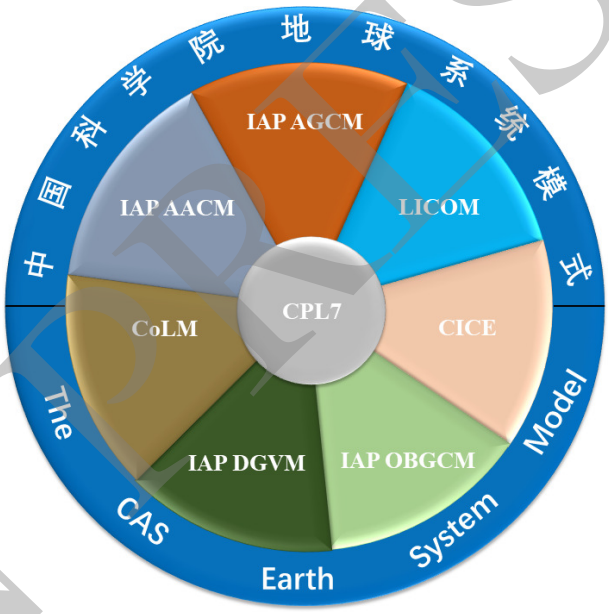

Fig. 1. The framework of CAS-ESM2.0 used in this study, with active carbon–climate interactions.

Table 1. Summary of the two emissions-driven simulations in this study.

Experiment name	Description	Anthropogenic forcings	Period
esm_piControl	Preindustrial control; CO_2 concentration calculated	CO_2 from both fossil fuel combustion and land-use change are prescribed to be zero	550 years
esm_historical	Historical simulation; CO_2 concentration calculated	Historical time-dependent CO_2 emissions, including fossil fuel combustion and land-use change	1850–2014

We configured each experiment with 512 cores at a horizontal resolution of 1.4° and a vertical resolution of 35 levels. The esm_piControl and esm_historical experiments took at least three months and one month to finish, respectively. Besides, we also spent more time debugging and calibrating the model results. Because of this expensive time cost, we did not conduct experiments with different resolutions to estimate the dependence of the model results on the resolution. Based on our previous experience, the resolution may affect the model results at a site scale, but it does not change the overall conclusion of the modeled results at regional and global scales.

3.2. *Data*

We used observational datasets from three sources. The annual mean CO_2 concentration for the period 1850–2014 comes from the CMIP6 input data (https://esgf-node.llnl.gov/search/input4mips/). We also obtained CO_2 observations for the sites of Mauna Loa (MLO) and Barrow (BRW) from NOAA Global Monitoring Laboratory measurements (Lan et al., 2023). These two sites have long-term, continuous records, and have been used as baseline observations in many previous studies (Graven et al., 2013; Forkel et al., 2016). In this study, we used their monthly observations during the overlapping periods of 1959–2014 (MLO) and 1972–2014 (BRW). Additionally, we downloaded the satellite product from GOSAT (Greenhouse Gases Observing Satellite; https://data2.gosat.nies.go.jp). This product has a horizontal resolution of 2.5°, a vertical resolution of 17 levels, and a temporal resolution of 6 h. The GOSAT product spans from March 2009 to October 2017, and this study used its datasets covering the period 2010–2014.

3.3. *Methods*

We converted the CO_2 output of CAS-ESM2.0 to the column-average mole fraction of CO_2 in dry air (XCO_2), which is consistent with the CMIP6 annual mean CO_2 data. XCO_2 is computed following the method in Buchwitz and Reuter (2016):

$$XCO_2 = \frac{\sum n_d c_{CO_2}}{\sum n_d},$$

where c_{CO_2} is the CO_2 concentration (in ppm) at each level of CAS-ESM2.0 and n_d represents the corresponding number of dry-air particles within the level, calculated as follows:

$$n_d = \frac{N_a \Delta p (1 - q)}{m_d g}.$$

Here, N_a represents the Avogadro constant ($6.022140857 \times 10^{23}$ mol^{-1}) and m_d is the molar mass of dry air (28.9644×10^{-3} kg mol^{-1}). Δp is the pressure difference (in hPa) between the top boundary and the bottom boundary of the level; q represents the specific humidity (in kg kg^{-1}) within the level; and g is the gravitational acceleration, which changes with height and latitude. This study assigns g as a constant value of 9.80665 m^2 s^{-2} because the model top is not very high (2.2 hPa).

For comparing the model output to site observations, we used the CO_2 concentration in the lowest level and selected values of all grid points covering a 1.5° × 1.5° radius around the two stations, MLO and BRW. Finally, four grid points were selected for each of the two stations and their values were averaged to compare with the observations at MLO and BRW, respectively. When comparing to the GOSAT product, we converted the model output at the pressure level that was consistent with the GOSAT product.

4. Results

We first show the global mean XCO_2 of CAS-ESM2.0 (red line) and the observations (black line) in Fig. 2a. It is to be expected that the global mean XCO_2 increases with time during the period 1850–2014. CAS-ESM2.0 shows a highly consistent XCO_2 profile with that of the observations, illustrating a strong ability of CAS-ESM2.0 to capture this increasing trend of XCO_2. For the year 2014, CAS-ESM2.0 reproduces XCO_2 with a value of 398.50 ppm, which is very similar to the observed value of 397.55 ppm, while the nine CMIP6 models simulate XCO_2 values ranging from 381 to 412 ppm (IPCC, 2021).

Figure 2b further shows the simulated net carbon fluxes for CAS-ESM2.0, with the purple, blue and green lines representing the fluxes from anthropogenic emissions, ocean and land, respectively. Positive values represent the release of carbon to the atmosphere, while negative values represent the absorption of carbon from the atmosphere. The increasing anthropogenic emissions with time are expected and are thought to be the main cause of the increasing XCO_2 in Fig. 2a. The magnitudes of negative net carbon fluxes in the ocean and on land are also generally increasing with time, indicating increasing carbon absorbed from the atmosphere by the ocean and land. This phenomenon has been confirmed by many observations and is called the CO_2 fertilization effect because of the increasing CO_2 concentration. For the last 15 years (2000–2014), CAS-

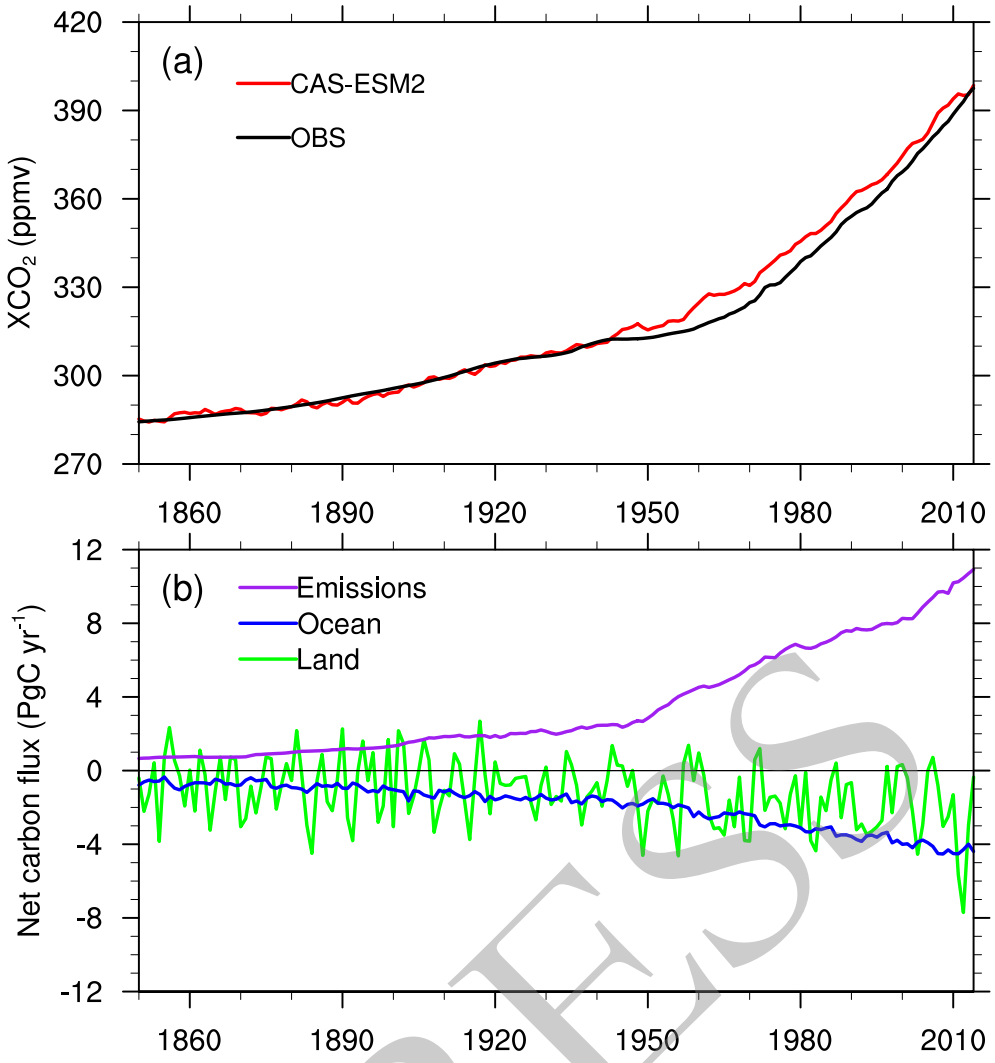

Fig. 2. Temporal evolution of (a) global mean XCO_2 (units: ppmv) and (b) net carbon flux (units: PgC yr^{-1}) during the period 1850–2014. The red and black lines in (a) represent CAS-ESM2.0 and observed values, respectively. The purple, blue and green lines in (b) represent the modeled net carbon flux from anthropogenic emissions, ocean and land, respectively.

ESM2.0 simulates net absorbed carbon fluxes, with average values of 2.23 and 4.19 PgC yr^{-1} for land and ocean, respectively. The magnitude of the net land carbon flux is similar to the estimation (2.81 PgC yr^{-1}) based on 17 DGVMs, while the magnitude of the net ocean carbon flux is larger than the estimation (2.32 PgC yr^{-1}) based on eight global ocean biogeochemistry models and seven ocean CO_2 data products (Friedlingstein et al., 2022). The larger net ocean carbon fluxes are partly caused by the non-equilibrium state of the ocean at the beginning, with approximately 1.0 PgC yr^{-1} of carbon absorbed. Moreover, CAS-ESM2.0 shows that the interannual variability of net carbon fluxes are larger for land than the ocean. This result agrees with nine CMIP6 models and observations and is reported in Chapter 3 of IPCC AR6 (IPCC, 2021).

In addition to the comparison at the global scale, we further compared the CAS-ESM2.0 results to site observations. Figure 3 shows the comparison at the two baseline sites, BRW and MLO, with the black and red lines representing the observed and modeled CO_2, respectively. Broadly, the simulated CO_2 concentration is similar to the site observations, with slightly higher magnitudes of 5.70 ppm (1.6% of the observation) and 5.16 ppm (1.5% of the observation) at sites BRW and MLO, respectively. In Fig. 3, the modeled CO_2 (red lines) is offset by these differences to provide a more intuitive comparison. Clearly, the temporal evolutions of the modeled CO_2 agree very well with those of the observations at the two sites, including the increasing trend and the seasonal cycle. In the year 2014, the modeled CO_2 concentrations at BRW and MLO are 399.84 and 398.02 ppm, respectively, which are very similar values to the observations (400.31 ppm and 399.81 ppm).

To examine the details of the seasonal cycle of CO_2, we compared CAS-ESM2.0 to the two site observations in each year and attached their climatological means in the bottom right of each panel in Fig. 3. Both the modeled and observed values

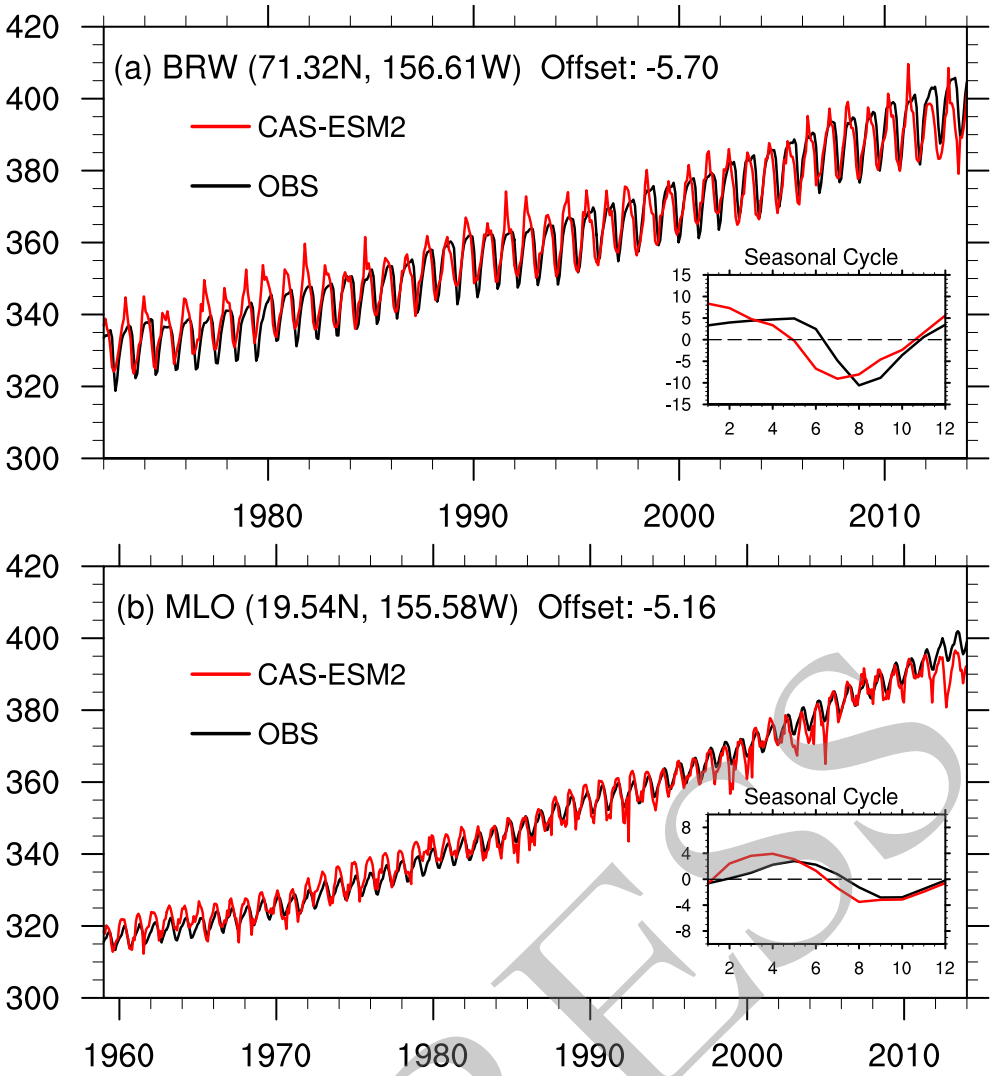

Fig. 3. Temporal evolution of CO_2 (units: ppm) at sites (a) Barrow (BRW) and (b) Manua Loa (MLO), with the climatological mean of the seasonal cycle of CO_2 attached in the bottom right of each panel. The red and black lines the represent CO_2 concentration of CAS-ESM2.0 and the observation, respectively. The modeled CO_2 is offset to have the same climatological mean as the observed CO_2, with the numbers shown in each panel. The seasonal values are calculated by subtracting the annual mean from their absolute values in each year.

are normalized by subtracting their respective annual mean values in each year. In this way, we can easily compare their profiles of the seasonal cycle of CO_2, including the time with the highest and lowest CO_2 and the seasonal cycle amplitude, and these comparisons are consistent with those based on absolute values.

At BRW, CAS-ESM2.0 simulated the time-averaged highest CO_2 in January and lowest CO_2 in July, while the time-averaged observation shows the highest CO_2 in May and lowest CO_2 in August. Besides, the modeled seasonal cycle amplitude of CO_2 (19.03 ± 3.32 ppm) is a little larger than that of the observed CO_2 (15.75 ± 1.47 ppm). At MLO, the modeled and observed CO_2 have a similar profile of the seasonal cycle of CO_2, while the modeled time with the highest (April) and the lowest (August) CO_2 are both one month ahead of the observed time. The simulated seasonal cycle amplitude of CO_2 (9.61 ± 2.73 ppm) is also larger than that of the observation (5.75 ± 0.45 ppm) at MLO. Overall, the modeled profiles of the seasonal cycle of CO_2 at the two sites are broadly similar to those of the observed CO_2, despite the aforementioned differences.

Figure 4 further compares the modeled seasonal cycle of CO_2 to that of the satellite CO_2 product at the regional scale. We plot the CO_2 in the lower levels of troposphere (below 500 hPa) over the Northern Hemisphere, which is characterized by prominent seasonal variability in CO_2. Broadly, CAS-ESM2.0 can capture the seasonal cycle of CO_2 reasonably well over the northern high latitudes, with lower values in boreal summer and higher values in boreal winter. This seasonal cycle of CO_2 is mainly caused by the seasonal variability in net land carbon fluxes, with net carbon uptake during boreal summer because of enhanced photosynthesis and net carbon release during boreal winter because of ecosystem respiration. The consis-

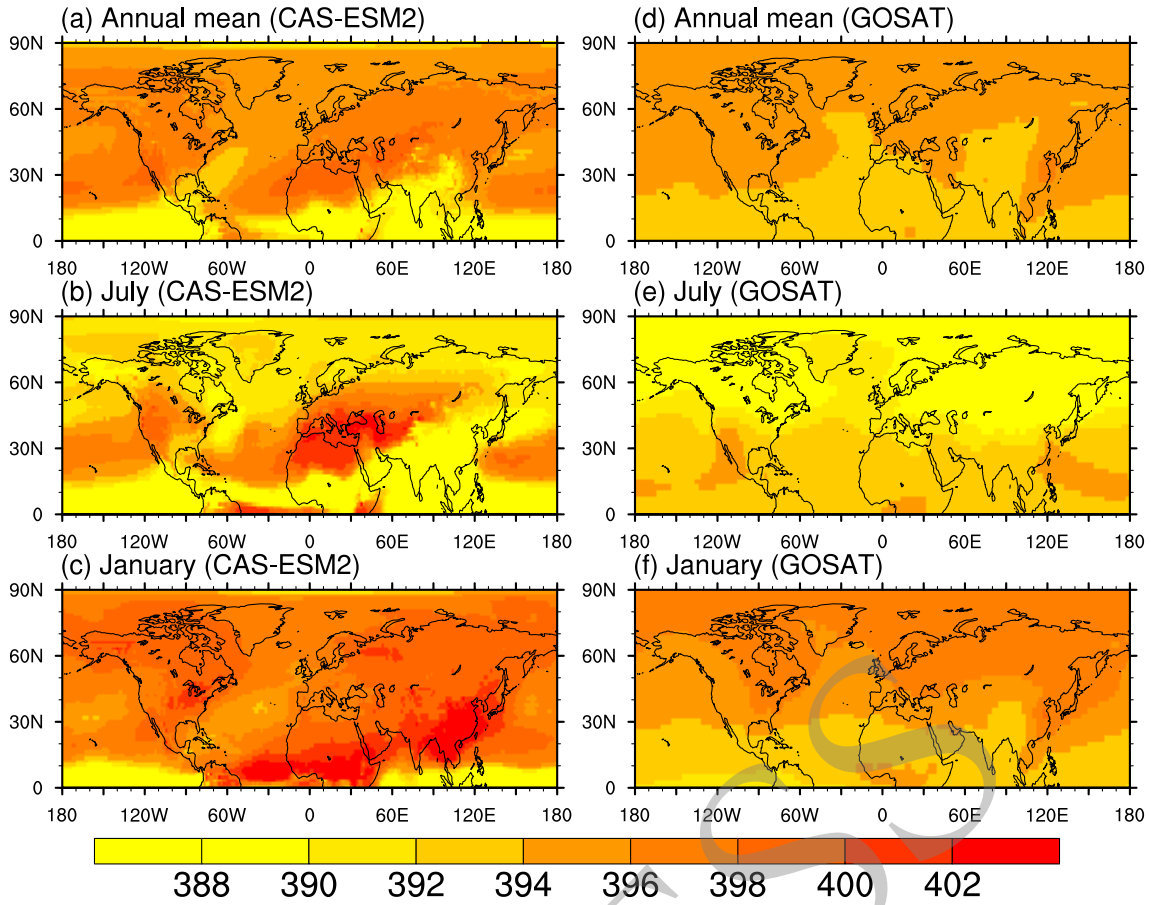

Fig. 4. Spatial distribution of low-level (below 500 hPa) CO_2 concentration (units: ppm) for the (a, d) annual mean, and the months of (b, e) July and (c, f) January, during the period 2010–2014. Panels (a–c) show the modeled results of CAS-ESM2.0, while panels (d–f) are from the GOSAT CO_2 product.

tency in the seasonal cycle of CO_2 between CAS-ESM2.0 and GOSAT means CAS-ESM2.0 can also reasonably reproduce the seasonal variability of the terrestrial carbon cycle.

Meanwhile, the patterns of the modeled CO_2 are different to those of GOSAT CO_2 products. Overall, CAS-ESM2.0 overestimated the CO_2 at most grid points of the Northern Hemisphere, relative to the GOSAT CO_2. This overestimation is larger in Central Asia and North America in July and at almost all grid points in January. To detect the possible causes of these biases, we analyzed the net terrestrial carbon fluxes (Fig. 5). In July, Central Asia and North America are mainly characterized by net carbon release from land to atmosphere, which may be caused by the modeled biases in terrestrial respiration. In January, the overall larger overestimation of CO_2 is partially caused by the fire carbon emissions accumulated over the whole year and released to the atmosphere on 1 January in the next year. These biases indicate that the modeled atmospheric CO_2 remains uncertain in many regions, and these uncertainties need to be reduced through more comprehensive detection.

5. Discussion and outlook

The main goal of this paper is to report the process of CAS-ESM2.0 in simulating atmospheric CO_2 and its two-way coupling with terrestrial and oceanic carbon cycles. The results are preliminary, and more comprehensive evaluations are necessary in the future to systematically understand the model performance. These future evaluations should apply more site observations of atmospheric CO_2 and carbon fluxes to/from the land and ocean. Comparison of CAS-ESM to such site observations will facilitate a comprehensive examination of the ability of the model in reproducing atmospheric CO_2, as well as the sources of model biases. For example, CAS-ESM2.0 overestimated the seasonal amplitude of atmospheric CO_2 at the two baseline sites (BRW and MLO). This overestimation may be caused by unrealistic net ecosystem production and fire carbon emissions. An application of observations of each carbon flux favors a comprehensive evaluation to accurately describe the corresponding processes. Additionally, there are an increasing number of satellite CO_2 products and CO_2 outputs from Earth system models that participate in the CMIP emissions-driven simulations. The potential availability of these CO_2 datasets will be favorable for examining the uncertainties of CAS-ESM in reproducing atmospheric CO_2 at the regional and global scale.

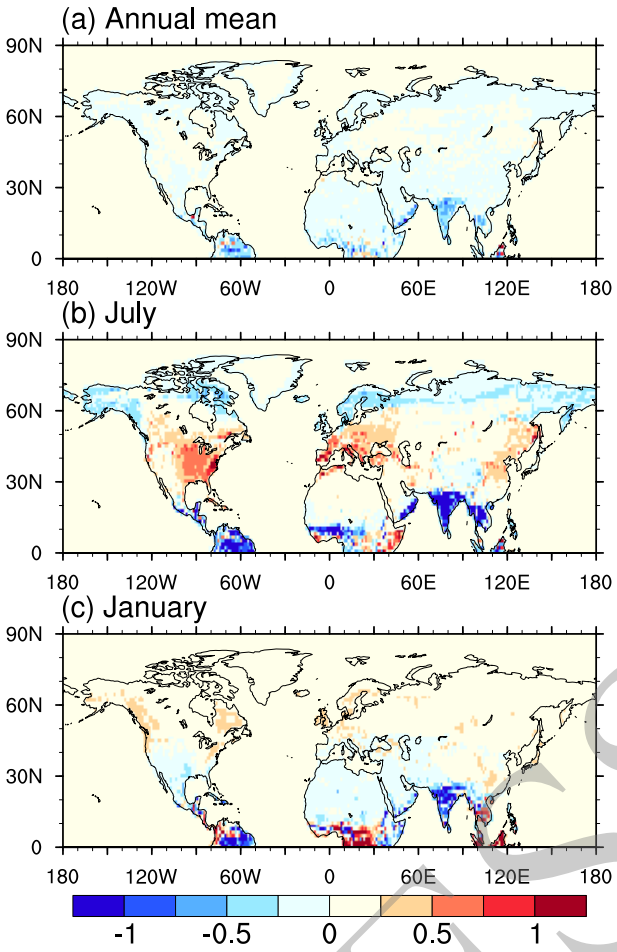

Fig. 5. Spatial distribution of net carbon fluxes in land (units: TgC) for (a) annual mean, (b) July and (c) January during the period 2010–2014. Positive values represent net carbon release from land to atmosphere, while negative values represent net carbon uptake from atmosphere to land.

Overall, we will focus next on comprehensively evaluating CAS-ESM2.0 with more and varied sources of observations and models for a better understanding of the behaviors of CAS-ESM and to further improvement its simulation of coupled carbon –climate interactions.

There are many potential applications of CAS-ESM once it has the ability to simulate CO_2–carbon–climate interactions. One significant area is the investigation of scientific issues associated with atmospheric CO_2. For example, previous studies have reported that the seasonal cycle amplitude of atmospheric CO_2 has increased by 50% since 1960s over the northern high latitudes (Graven et al., 2013; Forkel et al., 2016). However, most Earth system models underestimate this observed CO_2 seasonal amplitude and its trend (Graven et al., 2013; Gier et al. 2020). These model biases mean that many key processes remain uncertain and are even missing in many Earth system models (Arora et al., 2020). Using CAS-ESM and other Earth system models, we can try to quantify the causes of models biases associated with each specific process, such as fire and vegetation dynamics, as well as reveal the key underlying mechanisms.

Another important application of CAS-ESM is to support China's goal of carbon neutrality. China has set a target to achieve carbon neutrality by the year 2060. One key job of this goal is to accurately set a carbon-neutral pathway that is decided by many aspects, including anthropogenic emissions and net carbon fluxes from natural ecosystems. Using CAS-ESM with coupled carbon–climate interactions, we can estimate net carbon fluxes in China at each stage of the carbon-neutral process, and this estimation can be fed back to policymakers for adjustments to the carbon-neutral pathway. Moreover, CAS-ESM can also project climatic effects of the carbon-neutral goal, not only for China but also in combination with other countries. Overall, the implementation of CAS-ESM with fully coupled carbon–climate simulation is an important stage in the development of CAS-ESM, especially from the perspective of supporting China's goal of carbon neutrality.

6. Summary

A successful two-way coupling of atmospheric CO_2 with the climate and the carbon cycles of land and ocean in CAS-ESM2.0 has been reported in this paper. Using this version of the model, we conducted an emissions-driven CMIP6 historical simulation to examine its performance in reproducing atmospheric CO_2. The preliminary results show that CAS-ESM2.0 can reproduce the increasing trend of annual CO_2 during the period 1850–2014, and can capture the seasonal cycle of CO_2 at two baseline sites (MLO and BRW), as well as over northern high latitudes. These results illustrate that CAS-ESM2.0 has the ability to simulate CO_2–carbon–climate interactions, despite uncertainties remaining in the processes involved. In future work, we intend to conduct more comprehensive evaluations of the model by comparing its results with multiple sources of observations and other modeled outputs, and well as gain a systematic understanding the model's behaviors and detect the sources of uncertainties. Overall, this is an important stage of the development of CAS-ESM because it will provide significant scientific support for climate research and China's goal of carbon neutrality.

Acknowledgements. This study was supported by the National Key Research and Development Program of China (Grant No. 2022YFE0106500), the Youth Innovation Promotion Association of the Chinese Academy of Sciences (Grant No. 2022076), and the National Key Scientific and Technological Infrastructure project "Earth System Numerical Simulation Facility" (EarthLab; 2023-EL-ZD-00012).

REFERENCES

Arora, V. K., and Coauthors, 2020: Carbon-concentration and carbon-climate feedbacks in CMIP6 models and their comparison to CMIP5 models. *Biogeosciences*, **17**, 4173–4222, https://doi.org/10.5194/bg-17-4173-2020.

Buchwitz, M., and M. Reuter, 2016: Merged SCIAMACHY/ENVISAT and TANSO-FTS/GOSAT atmospheric column-average dry-air mole fraction of CO_2 (XCO_2) (XCO2_CRDP3_001), Technical Report, Version 1 (rev 2), 11 pp.

Eyring, V., S. Bony, G. A. Meehl, C. A. Senior, B. Stevens, R. J. Stouffer, and K. E. Taylor, 2016: Overview of the Coupled Model Intercomparison Project Phase 6 (CMIP6) experimental design and organization. *Geoscientific Model Development*, **9**, 1937–1958, https://doi.org/10.5194/gmd-9-1937-2016.

Feng, X., S. Wang, and Z. C. Niu, 2018: Variational characteristics of CO_2 concentrations and $\delta^{13}C$ values at the urban sites in Beijing and Xiamen, China. *Journal of Earth Environment*, **9**(4), 316–322, https://doi.org/10.7515/JEE182029. (in Chinese with English abstract)

Forkel, M., N. Carvalhais, C. Rödenbeck, R. Keeling, M. Heimann, K. Thonicke, S. Zaehle, and M. Reichstein, 2016: Enhanced seasonal CO_2 exchange caused by amplified plant productivity in northern ecosystems. *Science*, **351**, 696–699, https://doi.org/10.1126/science.aac4971.

Friedlingstein, P., and Coauthors, 2022: Global carbon budget 2021. *Earth System Science Data*, **14**, 1917–2005, https://doi.org/10.5194/essd-14-1917-2022.

Gier, B. K., M. Buchwitz, M. Reuter, P. M. Cox, P. Friedlingstein, and V. Eyring, 2020: Spatially resolved evaluation of Earth system models with satellite column-averaged CO_2. *Biogeosciences*, **17**, 6115–6144, https://doi.org/10.5194/bg-17-6115-2020.

Graven, H. D., and Coauthors, 2013: Enhanced seasonal exchange of CO_2 by northern ecosystems since 1960. *Science*, **341**, 1085–1089, https://doi.org/10.1126/science.1239207.

IPCC, 2021: Summary for policymakers. *Climate Change 2021: The Physical Science Basis. Contribution of Working Group I to the Sixth Assessment Report of the Intergovernmental Panel on Climate Change*, V. Masson-Delmotte et al., Eds., Cambridge University Press, Cambridge, UK.

Ji, D., and Coauthors, 2014: Description and basic evaluation of Beijing Normal University Earth System Model (BNU-ESM) version 1. *Geoscientific Model Development*, **7**, 2039–2064, https://doi.org/10.5194/gmd-7-2039-2014.

Lan, X., P. Tans, and K. W. Thoning, 2023: Trends in globally-averaged CO_2 determined from NOAA Global Monitoring Laboratory measurements. Version 2023-09 NOAA/GML.

Li, F., X. D. Zeng, and S. Levis, 2012: A process-based fire parameterization of intermediate complexity in a Dynamic Global Vegetation Model. *Biogeosciences*, **9**, 2761–2780, https://doi.org/10.5194/bg-9-2761-2012.

Xu, Y. F., Y. C. Li, and M. Chu, 2013: A global ocean biogeochemistry general circulation model and its simulations. *Adv. Atmos. Sci.*, **30**, 922–939, https://doi.org/10.1007/s00376-012-2162-0.

Ying, N., Q. Ye, and J. J. Xia, 2019: Interannual and seasonal cycles of CO_2 from GOSAT and AIRS. *IOP Conference Series: Earth and Environmental Science*, **237**, 022003, https://doi.org/10.1088/1755-1315/237/2/022003.

Zeng, X. D., F. Li, and X. Song, 2014: Development of the IAP dynamic global vegetation model. *Adv. Atmos. Sci.*, **31**, 505–514, https://doi.org/10.1007/s00376-013-3155-3.

Zhang, H., and Coauthors, 2020: Description and climate simulation performance of CAS-ESM version 2. *Journal of Advances in Modeling Earth Systems*, **12**, e2020MS002210, https://doi.org/10.1029/2020ms002210.

Zhu, J. W., and Coauthors, 2018: Evaluation of the new dynamic global vegetation model in CAS-ESM. *Adv. Atmos. Sci.*, **35**, 659–670, https://doi.org/10.1007/s00376-017-7154-7.